Histol Histopathol (2007) 22: 729-742

http://www.hh.um.es

Histology and Histopathology

Cellular and Molecular Biology

Identification of differentially expressed genes in fetal rat forebrain exposed to a teratogen by cDNA microarray analysis

S.T. Dheen, A.J. Hao, J. Fu, P. Gopalakrishnakone and E.-A. Ling

Molecular Neurobiology Laboratory, Department of Anatomy,

Yong Loo Lin School of Medicine, National University of Singapore, Singapore

Summary. In an attempt to understand the molecular basis underlying the neural tube defects induced by the teratogen, cyclophosphamide (CP), cDNA microarray analysis was carried out in neural tubes of embryos derived from normal and CP-treated rats. Genes found to have altered expression levels in CP-treated group were clustered into groups on the basis of their biological functions. The expression profile of different genes involved in transcription of molecules related to cell adhesion, inflammation, metabolism and neurotrophic factors pathways as well as in still undefined processes was differentially affected by the teratogen treatment. The most remarkable change was the up-regulation of genes related to an inflammatory process dominated by the fetal brain macrophages viz. amoeboid microglia. Amoeboid microglia/brain macrophage expansion, based on gene expression and histological analysis, was found to be vigorous at the subventricular region. The present results suggest that a vigorous inflammatory response involving amoeboid microglia/brain macrophages primarily is an important component in CP-induced prenatal development disorder.

Key words: Amoeboid microglia/brain macrophages, Inflammation genes, Fetal forebrain, Teratogen, Microarray

Introduction

Molecular genetic mechanisms that control morphogenesis during development are becoming increasingly important to the study of human embryology. It is clear that the functional disruption of some of the regulatory genes by mutation and actions of environmental or therapeutic teratogens produce a spectrum of congenital malformations in human embryos (Seller and Bnail, 1995; DeSesso et al., 1999; Al Deeb et al., 2000). The causes of these developmentally related anomalies including the neural tube defect (NTD) are variable and multifactorial. NTD is a complex and devastating disorder that affects the population and ranks the second among prevalent congenital disorders in the human. It includes anencephaly, exencephaly, and spina bifida (Ferm and Hanlon, 1986). Although it is widely accepted that the failure of closure of the neural tube is the basic cause of NTD, the hydromyelic theory suggests the possibility of the reopening of the closed neural tube and consequent NTD (Padmanabhan, 1988, 1990). Experimentally, NTD in the fetal rat can be induced by cyclophosphamide (CP). CP has previously been shown to produce cell death and induce a broad spectrum of anomalies including NTD in rodents. Rats exposed to 15mg/kg of CP on gestation day 13 exhibit obvious craniofacial anomalies i.e. exencephaly affecting about 99% of the fetuses (Ivnitsky et al., 1998; Padmanabhan, 1998, 1990). Neuropathological and neuroimaging studies have reported a number of forebrain morphological alterations associated with the NTD. Morphological changes such as apoptosis, decreased cell density and distortions in neuronal migration and organization have

Offprint requests to: Dr. S. Thameem Dheen, Molecular Neurobiology Laboratory, Department of Anatomy, Yong Loo Lin School of Medicine, National University of Singapore, Blk MD10, 4 Medical Drive, 117597 Singapore. e-mail: antstd@nus.edu.sg

Abbreviations: AM, amoeboid microglia; BM, brain macrophages; BTel, basal telencephalon; Btp, basal telencephalon plate; CP, cyclophosphamide; gro, growth-regulated oncogene; IL, interleukin; iNOS, inducible nitric oxide synthase; eNOS, endothelial nitric oxide synthase; MCP-1, monocyte chemotactic protein-1; M-CSF, macrophage clony stimulating factor; MIP-1α, ß, macrophage inflammatory protein-1alpha, beta; NGF, nerve growth factor; NT 3, neurotrophin 3; NTD, neural tube defect; RANTES, regulated upon activation normal T cell expressed and secreted; TGF-ß, transforming growth factor beta; TNF-α, tumor necrosis factor alpha; VCAM-1, vascular cell adhesion molecule 1; vnl, ventral neuroepithelium of diencephalon

been reported in ultrastructural and immunohistochemical studies, but the molecular bases underlying these disorders are poorly understood.

Changes in gene expression have been the subject of many studies of different processes involved in neural tube development. However, most of these studies have focused on a few gene products and, hence, the apparent lack of information of simultaneous expression of large numbers of genes at a specific point in time during development (Bennett et al., 2000; Craig et al., 2000; Hansen et al., 2001). Consequently, the complex gene expression patterns in the normal and abnormal fetal brain during development are not well understood. Recently, microarray technology has provided an opportunity for application of gene expression analysis to complex diseases (Eisen et al., 1998; Brown and Botstein, 1999; Alizadeh and Staudt, 2000), and the approach has been successfully used in addressing fundamental biological questions in various diseases including human cancer (Alizadeh et al., 2000). However, due to the inherent complexity of nervous tissue, a very few microarray studies of the central nervous system (CNS) have been conducted (Whitney et al., 1999; Chabas et al., 2001; Grunblatt et al., 2001; Jin et al., 2001; Mody et al., 2001; Pasinetti, 2001) especially in the fetal CNS. In the latter, it may be attributed to the need to utilize embryo materials. In contrast to adult and cancer tissues, where many biological measures reveal differences of several orders of magnitude, certain genes may not be expressed at all in the embryo during normal development. Furthermore, gene alterations in abnormal fetal brain may appear to be much more moderate compared to the adult tissue. In order to determine whether there are modest, but consistent changes in gene expression in the fetal brain following CP treatment, we designed a two-step experimental approach. First, we used cDNA microarrays to compare the relative expression levels of 1080 gene transcripts in the normal and CP-treated fetal brain. These data were analyzed by gene expression profiling of over 150 gene groups, including custom-designed cascades of gene products related to specific nervous system functions. To confirm the microarray results, which indicated augmented expression of genes related to a macrophage/ microglia mediated inflammatory response, we measured the relative expression of a subset of these genes by RT-PCR and in situ hybridization. Implications drawn from these changes in gene expression may provide insights into the etiology of the NTD.

Materials and methods

Animals

Sprague-Dawley rats (Laboratory Animal Center, National University of Singapore) were used in this study. Timed mating was carried out by placing 3-4 females with a male rat overnight. The day of finding sperm in the vaginal smear was designated as embryonic day 0 (E0). A single dose (15 mg/kg) of CP (Sigma, Cat. No. C7397), freshly prepared in saline was administered intraperitoneally to groups of rats at E13 (Padmanabhan 1990). Control rats were injected with an equal volume of vehicle. At 48 h after CP treatment (E15), fetuses were collected following a Caesarean section of the mother rat anaesthetized with 7% chloral hydrate. In the handling and care of all animals, the International Guiding Principles for Animal Research, as stipulated by the World Health Organization (1985) and as adopted by the Laboratory Animal Center, National University of Singapore, were followed. For RNA preparation, the fetal forebrains were rapidly immersed into liquid nitrogen and stored at -80°C until the RNA isolation. For immunohistochemistry, the brains were fixed in toto in a fixative composed of 2% paraformaldehyde in 0.1 M phosphate buffer at pH 7.4 overnight at 4°C and cryoprotected by immersion in 20% sucrose in phosphate buffer. Coronal serial sections of the brain were cut at 30 µm thickness with a cryostat.

RNA preparation for microarray

Fetal forebrain RNA was isolated from 36 fetuses, each from 6 normal and 6 CP-treated mother rats, respectively (n=6). At 48 h after CP treatment, the brains from fetuses were rapidly removed, frozen in liquid nitrogen and kept at -80°C freezer until RNA extraction. Total RNA was extracted from the fetal forebrain by using AtlasTM Glass total RNA Isolation Kit (Cat No. K1036-1, Clontech, USA). The purity and quantity of RNA were determined by agarose gel electrophoresis (visual absence of 28S and 18S band degradation) and by spectrophotometry.

cDNA microarray analysis

The total RNA samples (20 µg) isolated from fetal brains of normal and CP-treated rats were reverse transcribed and labeled with Cy5 and Cy3 fluorescent dyes, respectively, using the Atlas^{TM} Glass Fluorescent Labeling Kit (Cat No. K1037-1, Clontech, USA). Following purification using NucleoSpin Column (Clontech, USA), the labeled probes were hybridized to the Rat Glass Microarray 1.0 (Cat No. 7902-1, Clontech, USA). Briefly, the labeled probe (80 ml) was mixed with the pre-warmed (50°C) GlassHyb Hybridization Solution (Clontech, USA) and then transferred to the Hybridization Chamber containing Rat Glass Microarray slide for hybridization overnight at 50°C in an upright position.

The array slide was removed from the Hybridization Chamber and incubated in wash solutions. Then the slide was rinsed briefly with distilled water, placed in a dry Wash Container and centrifuged briefly for drying the slide. The image was scanned with ScanArray 5000 (GSI Lumonics, USA) and analyzed by Quantarray software (GSI Lumonics, USA). The normalized data

list including the signal intensity on filter A and B were then reformatted and imported into a Microsoft Excel.

From the data obtained, the following criteria were used to define candidate genes that were differentially expressed between the control and experimental groups (Mirnics 2001). 1. A ratio between Cy3 and Cy5 of 1.5 or high; 2. Signal to background ratio greater than 2.0. The experiment was duplicated by reversing the labeling assignments of the sample and the average was used as the gene density. Fluorescent intensities normalized to the housekeeping genes spotted on the array were expressed as ratio of Cy3/Cy5. By this method, a total of 800 genes was found to have altered fluorescent intensities and genes listed in Table 1 were selected for further analysis.

RT-PCR analysis of differentially expressed genes

Total RNA was extracted from dissected fetal forebrain tissues using RNeasy Mini Kit (QIAGEN, Cat. No. 75161) according to the manufacturer's instructions and quantified spectrophotometrically. A total of 36 embryos from 6 mother rats for each experimental group was used (n=6). Reverse transcription and PCR were carried out sequentially in the same tube using One Step RT-PCR Kit (QIAGEN, Cat. No.210210). The respective fragments corresponding to the rat cDNA were amplified using the specific forward and reverse primers and the thermal profiles as given in Table 2. As an internal control for the RT-PCR, 528bp fragment of rat GAPDH was also amplified.

The number of amplification cycles was optimized to ensure that PCR products were quantified during the exponential phase of the amplification. In this experiment, 2 µg of total RNA was reverse transcribed in a 50 µl reaction volume. A 10 µl aliquot of each PCR product was size-separated by electrophoresis on a 2% ethidium bromide-containing agarose gel and photographed under the UV light. All photographed PCR products were scanned and analyzed by using NIH Image software. For respective samples, the PCR product values were normalized to the GAPDH PCR product values.

In situ hybridization

The fetal brains were fixed for 24h at 4°C in 4% paraformaldehyde and cryoprotected by immersion in

Table 1. Genes differentially expressed in CP-treated fetal forebrain.

Fold	Gene	Acc. No
Cell adhesion receptors/proteins		
3.3	Integrin-associated protein form 4	AF017437
3.5	Chondroitin sulfate proteoglycan 5 (neuroglycan C)	U33553
1.8	Integrin, beta 4	U60096
3.4	Cell surface glycoprotein CD44 (hyaluronate binding protein)	M61875
5.4	E-selectin; endothelial leukocyte adhesion molecule 1 (ELAM-1); leukocyte-endothelial cell adhesion	L25527
2.2	Cadherin; proton-driven peptide transporter	X78997
1.5	Vascular cell adhesion molecule 1	M84488
Growth factor, cytokine, chemokine & receptor		
1.5	Tumor necrosis factor superfamily, member CD30	D42117
1.5	Tumor necrosis factor receptor	M63122
2.3	Interleukin 6 receptor	M58587
2.1	Interleukin 2 receptor, alpha chain	M55049
1.6	Colony stimulating factor 1 receptor	X61479
1.5	Tumor necrosis factor alpha (TNF-alpha; TNFA); cachectin	X66539
1.5	Granulocyte-macrophage colony-stimulating factor (GM-CSF); colony-stimulating factor (CSF)	U00620
1.5	Macrophage inflammatory protein 2 (MIP2)	U45965
1.8	Small inducible cytokine subfamily A member 3 (SCYA3); macrophage inflammatory protein 1 alpha (MIP1-alpha; MIP1A)	U22414
1.7	Transforming growth factor beta-1 gene	S77492
-2.4	Nerve growth factor receptor, fast	X05137
-2.6	Insulin-like growth factor 2 receptor	U59809
-2.5	Chemokine (C-X-C) receptor 2	X77797
-1.6	Beta-nerve growth factor (beta-NGF; NGFB)	M36589
-1.7	Macrophage migration inhibitory factor (MIF); glutathione-binding 13-kDa protein	U62326
-3.5	Fibroblast growth factor 2	M22427
-1.6	Neurotrophin 3 (NTF3); neurotrophic factor; HDNF; nerve growth factor 2 (NGF2)	M34643
-1.7	Neurotrophin 5 (neurotrophin 4/5)	S69323
Metabolism		
1.6	Inducible nitric oxide synthase (iNOS); type II NOS (NOS2)	D14051
-3.3	Nitric oxide synthase 3 (NOS3); endothelial NOS (eNOS)	U02534
-2.1	Neuron-specific enolase (NSE); gamma enolase; 2-phospho-D-glycerate hydrolyase	AF019973
Protease		
1.5	Cathepsin D	X54467
1.6	Matrix metalloproteinase 11 (stromelysin 3)	U46034
1.8	Gelatinase A	U65656
1.6	Cathepsin K	AF010306
1.7	Cathepsin B	X82396
1.7	Interleukin 1beta converting enzyme /caspase 1	U14647

20% sucrose in phosphate buffer. Coronal serial sections (15 µm thick) of the forebrain were cut with a cryostat and mounted on 3-aminopropyl triethoxy-silane coated slides. Antisense oligonucleotide probes for rat iNOS, rat CSF-1R, rat M-CSF and rat caspase-1 were prepared using specific sequences as given in Table 3. Only for rat iNOS, a cocktail of two oligonucleotide probes was used for in situ hybridization. The oligonucleotides were labeled at the 3' end with DIG-dUTP/dATP using the DIG Oligonucleotide Tailing Kit (Roche, Boehringer Mannheim, Cat No: 1417231). The sections were washed in PBS buffer, exposed to proteinase K (1 µg/ml) (GER, Mannheim, Cat. No. 754723) and fixed in 4% ice-cold paraformaldehyde (PF). Prehybridization with hybridization solution (DAKO, Cat. No. S330510) was performed for 2 h at 42°C. Hybridization was carried out with the labeled probe (1µg/ml of hybridization solution) in a humidified chamber at 42°C overnight. After hybridization, the sections were washed at 42°C with 2xSSC (3M NaCl, 0.3M Na-citrate, pH 7.0) for 2h with 4-6 changes and in 0.2xSSC for 1 h at room temperature with 3 changes. The hybridization signal was detected by anti-digoxigenin conjugated with alkaline phosphatase followed by incubation in the NBT/BCIP color substrate solution (Roche, Boehringer Mannheim, Cat. No. 1681451). The sections were fixed with 4% PF, mounted with glycerol and coverslipped for analysis on a Zeiss microscope. As a control, adjacent sections were hybridized with the corresponding sense oligonucleotide probe. Alternatively, some sections were digested with RNase before hybridization.

Lectin histochemistry

Identification of amoeboid microglia (AM)/brain macrophages (BM) was carried out using the peroxidase-conjugated *Griffonia simplicifolia* B4 isolectin (Sigma, L5391) dissolved in 0.1M phosphate buffer saline (PBS, pH 7.4). The sections were incubated with it overnight at 4°C and reacted with nickel-enhanced diaminobenzidine and counterstained with methyl green.

For quantitative analysis, immunolabeled cells in btp, BTel and vnl as outlined in Fig. 3A were identified and counted under a x 20 objective using an Aristoplan microscope. The number of cells was normalized to the total area of btp, BTel and vnl as determined with the image analysis system (Image-Pro plus version 4.1), yielding the cell density of microglial cells. Results are expressed as cells per square millimeter ± SD. A total of 15 sections, 3 each from 5 rats, was examined and the crude cell counts were averaged and analyzed. Student's

Table 2. Primer sequence and fold changes of gene expression as measured by RT-PCR.

mRNA	Primer sequence (5'—3')	Annealing(°C, S)	Cycles	Size(bp)	Fold (n=6)
NT 3	F: tttcttgcttatctccgtggcatcc; R: ggcagggtgctctggtaattttcct	57, 30	28	167	-1.6
ICAM	F: aggtatccatccatcccaca; R: gccacagttctcaaagcaca	54, 60	30	210	1.7
TNF-α	F: cccagaccctcacactcagat; R: ttgtcccttgaagagaacctg	55, 30	30	215	Induced
TGF-ß1	F: gagagccctggataccaactactg; R: gtgtgtccaggctccaaatgtag	55, 30	30	173	Induced
VCAM	F: ctgacctgctcaagtgatgg; R: gtgtctccctctttgacgct	54, 60	30	260	1.5
MIP2	F: gttgttgtggccagtgagctgcg; R: gttagccttgcctttgttcagtat	60, 40	32	219	1.7
gro	F: gcgcccgtcgccaatgagctgc; R: cttggggacacccttcagcatcttttgg	60, 60	32	216	1.7
MIP1α	F: actgagctggaactaaatgc; R: aatgtgccctgaggtctttc	60, 60	32	282	1.8
MIP1ß	F: atgaagctctgcgtgtct; R: tcagttcaactccaagtc	60, 60	32	279	1.7
RANTES	F: accgtcatcctcgttg; R: ctctgggttggcac	60, 60	32	207	Induced
Caspase1	F: cacgtcttgccctcattatc; R: ctgtcagaagtcttgtc	51, 60	32	245	Induced
nNOS	F: gacatcattctcgcagtcaa; R: gtctccagatgtgtagtgaa	55, 30	30	143	No difference
iNOS	F: ctcactgggactgcacagaa; R: tgttgaagggtgtcgtgaaa	54, 45	35	127	Induced
eNOS	F: tccagtaacacagacagtgca; R: caggaagtaagtgagagc	54, 45	32	693	-2.0
MIF	F: ccatgcctatgttcatcgtg; R: gaacagcggtgcaggtaagtg	54, 60	30	381	-1.6

Table 3. Antisense oligonucleotide sequence used for *in situ* hybridization.

Gene	Antisense Oligonucleotide Sequence	GeneBank Accession No
Rat iNOS	Probe I: 5' cat ttc ttc ctg ata gag gtg gtc ctc ctc tgg gtg cct gca 3' probe II: 5' tga gga agt atg agg ggc caa aag gaa aga gaa tgt g 3'	U03699.1
Rat CSF-1R	5'- gtt cat gg tgg ccg tgc gtg tgc caa cat cat tgc tgg cca cac aag a - 3'	X61479
Rat M-CSF	5'- ctc tgt tga ctc gag ggt ctg gca ggt act cct ggg cgg tcg ctg ctt ag-3'	023981
Rat caspase-1	5'-ata ccc cag atc ctg cag cag caa ctt cat ttc tct gag gtc aac atc a-3'	NM012762

t-test was performed to evaluate statistical significance ($P<0.01$).

Immunohistochemistry

Frozen serial sections of the rat brain from E15 fetuses were mounted on gelatinized slides. After blocking the endogenous peroxidase with 0.5% H_2O_2, the tissue sections were incubated with the primary antibodies, GFAP (SIGMA, Cat. No. G3893), and NG2 (Chemicon, Cat. No. AB5320) for detection of astrocytes and oligodendrocyte progenitor cells, respectively. Subsequent antibody detection was carried out using biotinylated anti- mouse IgG and reagents from ABC kit (Vector Laboratories, Cat. No. PK-400). The peroxidase reaction was visualized using 3, 3'-diaminobenzidine (DAB, Sigma, Cat. No. D-5637) as a peroxidase substrate. The reaction product was intensified with ammonium nickel sulphate. Tissue sections were finally counterstained with 1% methyl green, dehydrated in alcohol and mounted in Permount mounting medium (Biomeda, USA).

Confocal microscopy

For Mash-1, eNOS and VCAM-1 staining, the tissue sections were incubated with the primary antibody directed against MASH1 (BD Biosciences, Cat No. 556604), eNOS (Santa Cruz, Cat No. SC-8311) and VCAM-1 (Santa Cruz, Cat No. sc-1504). Subsequent antibody detection was carried out using FITC-conjugated secondary antibody and examined under a Carl Zeiss LSM410 confocal microscope.

Double-immunofluorescence labeling study was also carried out between different primary antibodies directed against TNF-α (R&D, AF-510-NA), TGF-ß (Santa Cruz, Cat No, sc-146), VCAM-1 and OX-42 (Sera-Lab, Cat. No. MAS 370b, 1:100) or Mash-1, NG2, and vimentin (Chemicon, Cat. No CBL202). In this study, two different primary antibodies were applied simultaneously. Subsequent detection of primary antibodies was carried out using fluorochrome-conjugated secondary antibodies and examined under a Carl Zeiss LSM410 confocal microscope.

Results

A large-scale gene expression analysis in the fetal forebrain exposed to CP by microarray

Genes found to have altered expression levels in brains of CP-treated groups in comparison with that of control samples by microarray analysis were clustered into groups based on their biological functions as listed in Table 1. The group of genes which showed up-regulated expression is dominated by the inflammation related genes. Many of these genes such as cytokines (TNF-α, TGF-ß), enzymes (iNOS) and protease (cathepsin, interleukin-1ß converting enzyme) are primarily expressed by the macrophage/ microglia lineage. The genes that are down regulated by more than 1.5 fold include mainly neurotrophic factors (NT 3, NT 4/5, NGF2, NGFB, FGF2).

RT-PCR analysis of inflammation related genes in the fetal forebrain exposed to CP

In order to confirm and validate the microarray results that showed the differential expression of genes related to inflammatory response, we measured the relative expression of a subset of these genes in the fetal forebrain of control and CP treated fetuses by RT-PCR (Table 2). Representative RT-PCR analyses confirm the microarray results which revealed the altered expression of various subsets of genes in the CP-treated fetuses. GAPDH was included in the analysis as an internal standard (Fig. 1). Each of the genes listed in Table 2 shows either an increase or a decrease of expression in CP-treated group compared with the controls. RT-PCR analysis of gene expression was further extended to other inflammation related genes such as ICAM-1, gro and RANTES. As shown in Table 2, the expression levels of these genes were also augmented when compared with the corresponding controls.

Localization of mRNA expression of iNOS, M-CSF, M-CSFR, caspase-1 in the fetal forebrain exposed to CP by in situ hybridization

The elevated expression of iNOS, M-CSF, MCSF-R, caspase-1, as revealed in microarray analysis, was

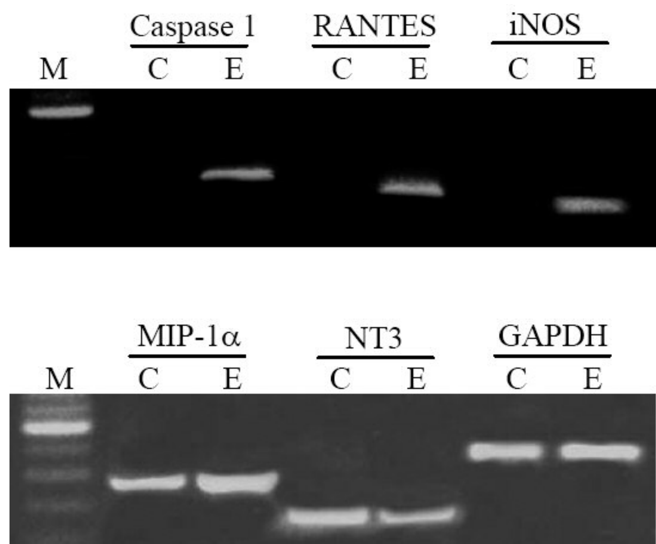

Fig. 1. Representative RT-PCR analyses confirming microarray results in which several genes are differentially expressed in control and CP-treated fetal brain (n=6). GAPDH was used as an internal standard. The expression of caspase-1, RANTES, and iNOS mRNA is undetectable in control group but is induced in CP-treated fetal brain. The expression of MIP-1a is increased and that of NT 3 is decreased. Data analysis is shown in Table 2. M: Size marker; C: control group; E: experimental group.

further analyzed by *in situ* hybridization. iNOS expression which was undetectable in the control group (Fig. 2A) was induced in the fetal forebrain exposed to CP (Fig. 2B). Although in the control group, weak expression of M-CSFR was detectable in cells that were distributed in the neuroepithelium associated with the lateral and the third ventricles, it was difficult to identify the cell types (Fig. 2C). In CP-treated group, M-CSFR expression was induced markedly in cells of the neuroepithelium associated with the lateral and the third ventricles (Fig. 2D). In addition, the mRNA expression of M-CSF (Fig. 2E) and caspase-1 (Fig. 2G) was hardly detectable in the control group. However, expression of these genes in the CP-treated group was significantly

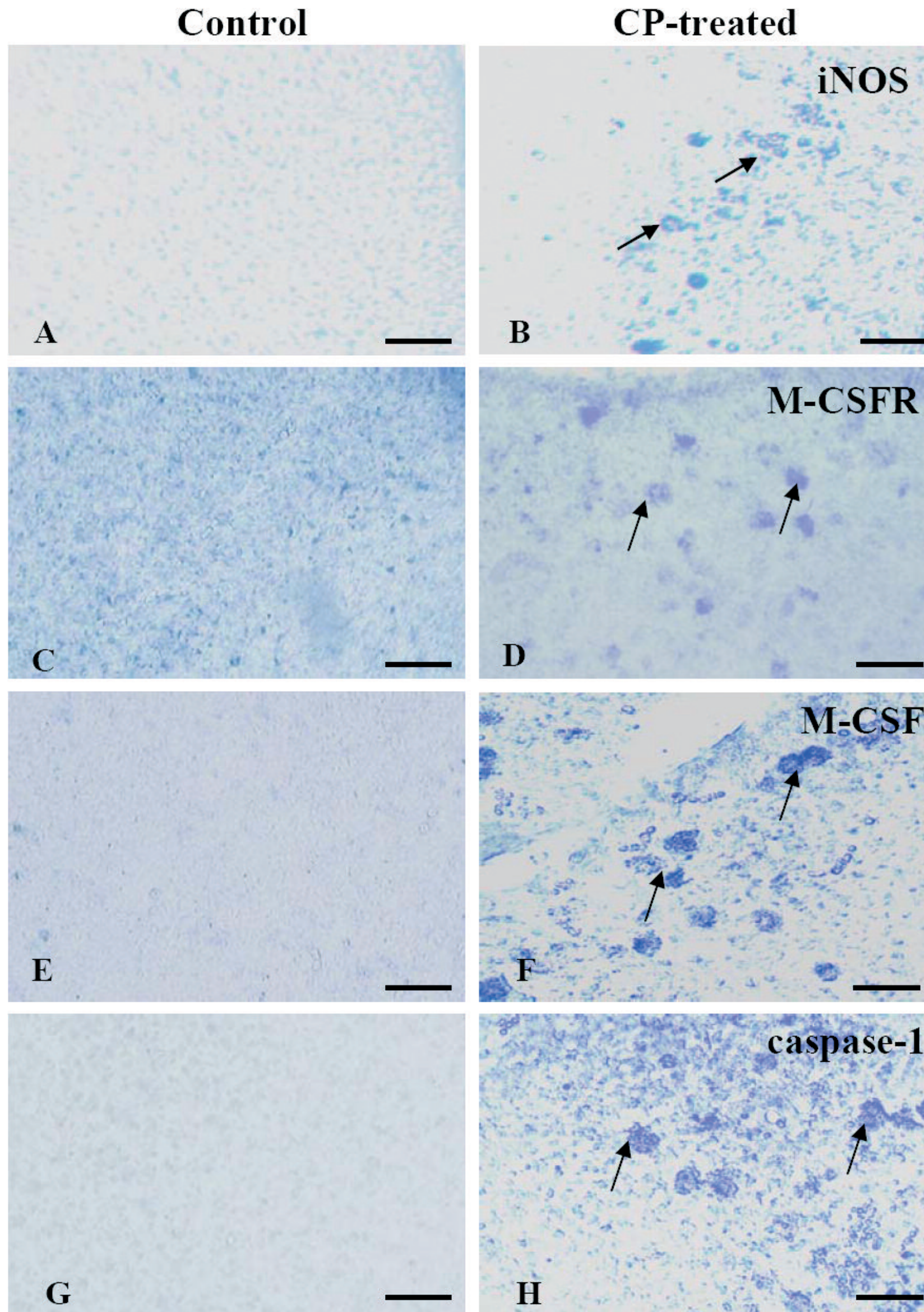

Fig. 2. Expression of iNOS, M-CSFR, M-CSF, and caspase-1 mRNA in the fetal brain by in situ hybridization. Note the lack of iNOS mRNA expression in the fetal brain of the control group **(A)**. In the dorsal neuroepithelium of diencephalon, the expression of iNOS mRNA is evident at 48h after exposure to CP (arrows, **B**). In the control group, the mRNA expression of M-CSFR is detectable but the identification of cell types was difficult (**C**). In CP-treated group, there is a marked increase in M-CSFR expression (arrows) localized in the neuroepithelium associated with the lateral and the third ventricles (**D**). In the control group, mRNA expression of M-CSF (**E**) and caspase-1 **(G)** is hardly detectable. The numerical densities of mRNA expression of M-CSF (arrows in **F**) and caspase-1 (arrows in **H**) in the btp are significantly higher than the corresponding areas in the control groups. Scale bar: 100 µm.

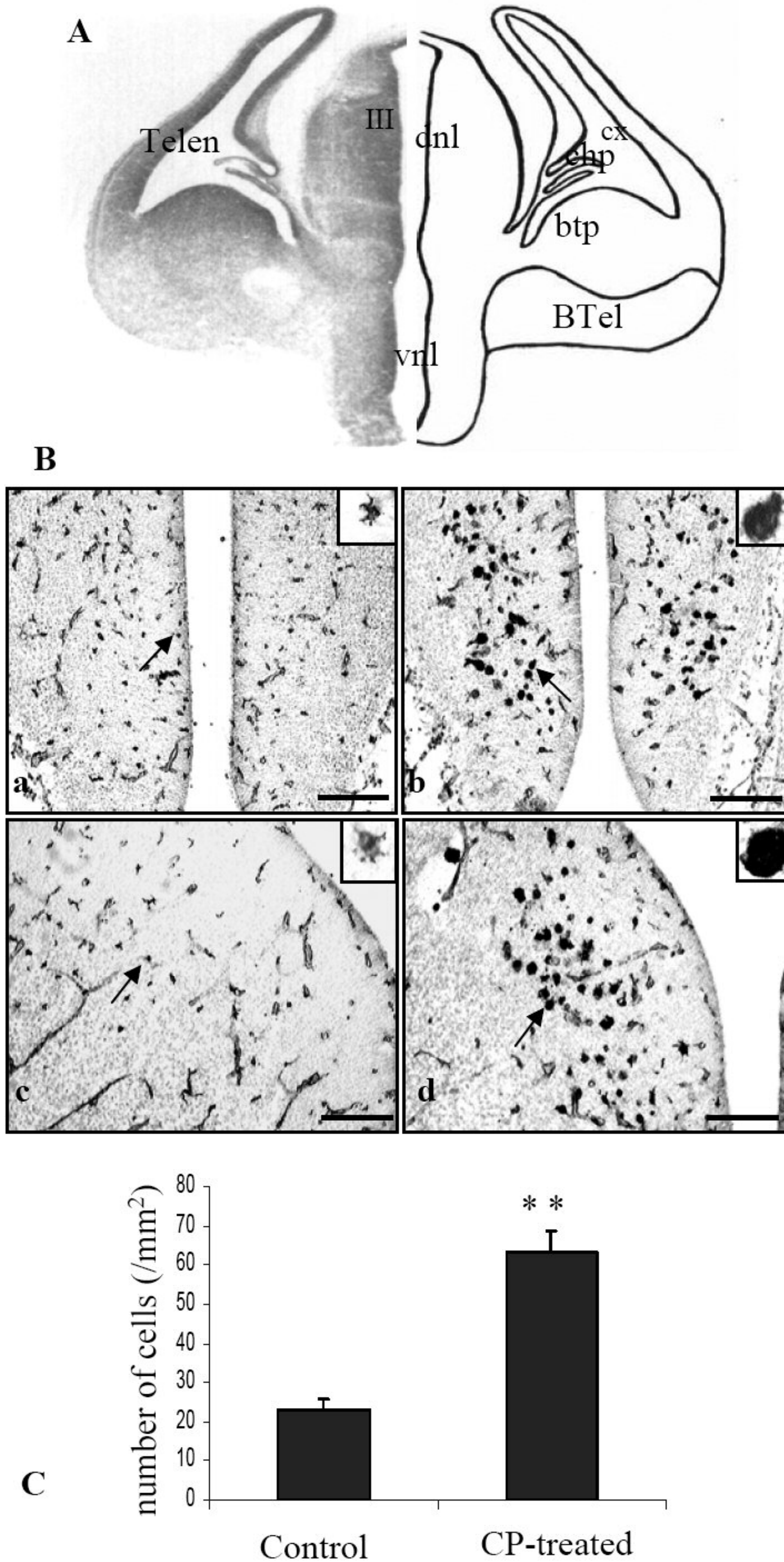

Fig. 3.A. A representative section of the fetal rat forebrain, delineating the anatomical regions for the present analysis. BTel, basal telencephalon; btp, basal telencephalon plate; chp, choroid plexus promordium; cx, cortical neuroepithelium; dnl, dorsal neuroepithelium of diencephalon; E15, embryonic day 15; Telen, telencephalon; vnl, ventral neuroepithelium of diencephalon; III, third ventricle. **B.** Distribution of amoeboid microglia (AM)/ brain macrophages (BM) in normal (a, c) and CP-treated (b, d) fetal forebrains. Inset is the enlarged view of the lectin positive cell indicated with an arrow in corresponding panel. In the control groups, isolectin labeled AM/BM (arrows) are ovoid or process bearing in the dorsal neuroepithelium of diencephalon (a) and basal telencephalon plate (c). At 48h after CP treatment (b, d), numerous isolectin labeled AM/BM (arrows) are detected in the dorsal neuroepithelium of diencephalon (b) and basal telencephalon plate (d). They are hypertrophic and are characterized by their amoeboidic appearance. Scale bar: 100 µm. **C.** The numerical densities of lectin positive cells in the btp, dnl and vnl as delineated in figure 3A. The value in each column represents mean density ± SD (n=6). Note the significant increase in number of microglia in CP-treated group compared with the corresponding control group. **: $p<0.01$.

induced (Fig. 2F, H) in the btp, as delineated in Fig. 3A. Sense probe showed the absence of any hybridization signal (data not shown).

Analysis of distribution of microglia in the fetal forebrain exposed to CP by lectin histochemistry

The distribution of microglia in the fetal forebrain was examined at 48h after the teratogen treatment. A representative section of the fetal rat forebrain (E15) delineating the anatomical regions for the present analysis is shown in Fig. 3A. AM/BM labeled with isolectin (Fig 3B. a, c) are ovoid or process bearing in the dorsal neuroepithelium of diencephalon (a) and basal telencephalon plate (c). At 48h after CP treatment, the microglial cells responded vigorously as manifested by the hypertrophy and numerical increase of the cells (b, d). The numerical densities of lectin labeled cells in the

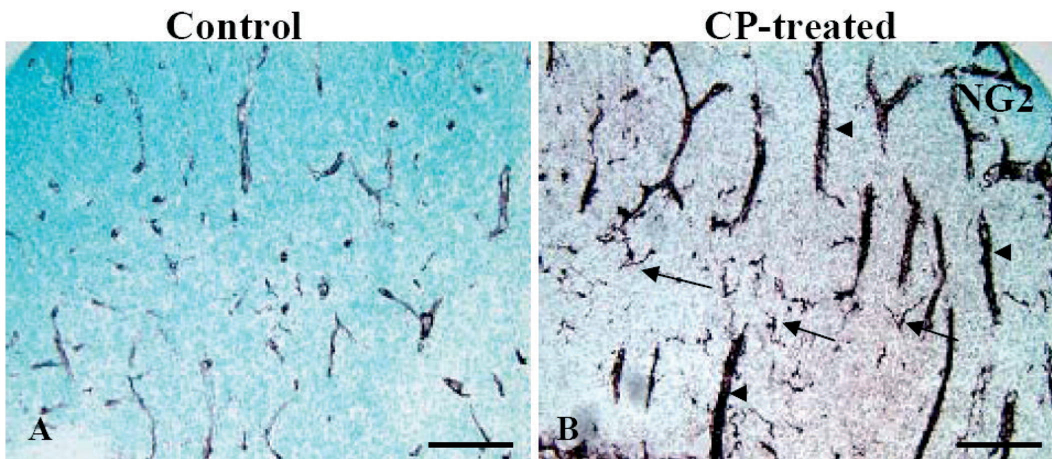

Fig. 4. Distribution of NG2-positive oilgodendrocyte progenitors in the fetal forebrain. With NG2 staining, oilgodendrocyte progenitor cells in the control group in the btp exhibit a small sized cell body **(A)**. At 48h after CP treatment, the oligodendrocyte progenitors exhibit very fine processes and increase in cell numbers (**B**). Blood vessels (arrow-heads) are also stained because of the presence of NG2 antigen in endothelial cells. Scale bar: 100 µm.

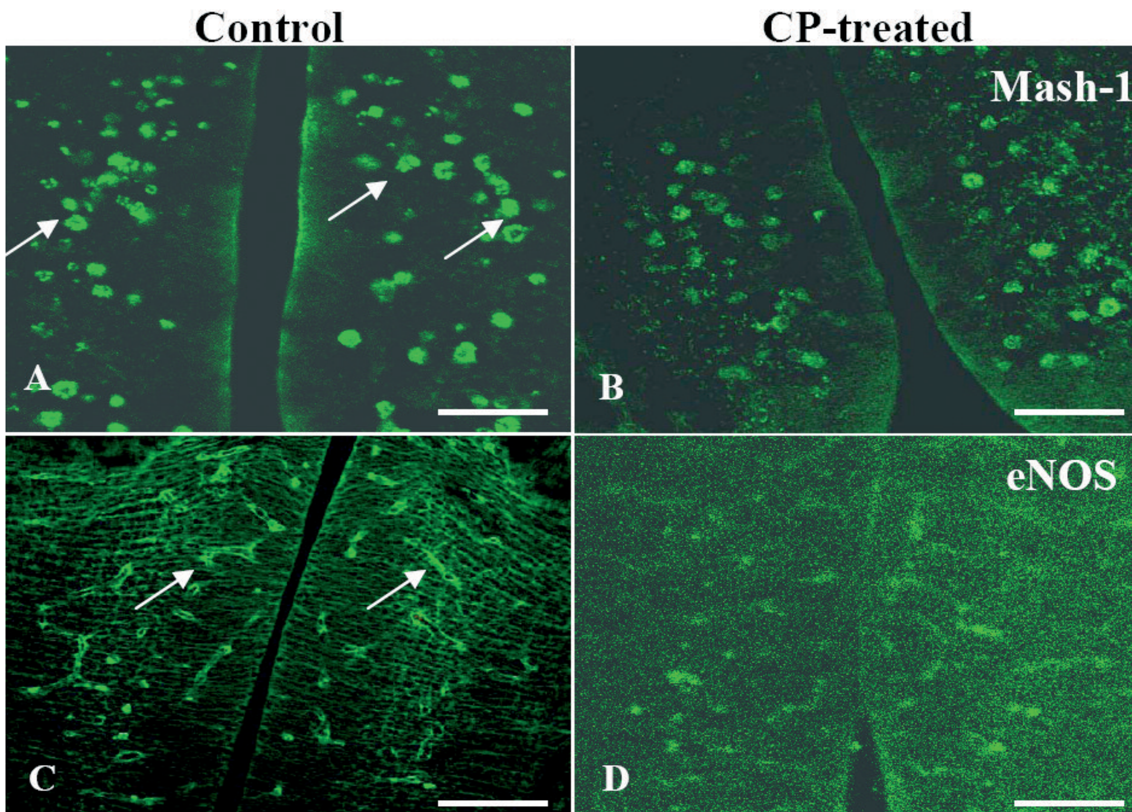

Fig. 5 Immunohistochemical analysis of Mash-1 and eNOS. In normal fetal brains, Mash-1 is detectable in the neuroepithelium associated with the lateral and the third ventricles (arrows in **A**). After CP treatment, Mash-1 staining appears to be reduced (**B**). In normal fetus, eNOS immunolabeling is distributed in the blood vessels around the third ventricle (arrows in **C**). After CP treatment, the eNOS staining appears to be reduced (**D**). Scale bars: 25 µm (A, B); 100 µm (C, D).

btp, dnl and vnl were significantly higher than the corresponding areas in the control groups (Fig. 3C).

Localization of astrocytes and oligodendrocytes in the fetal forbrain exposed to CP by immunohistochemistry

The distribution of astrocytes in the fetal forebrain (E15) was examined at 48h after the teratogen treatment. GFAP, a marker for astrocytes was undetectable in the forebrain of both groups at this stage. However, the staining of GFAP could be detectable at E18 and became more obvious after E19 (data not shown). The distribution of oligodendrocytes in the fetal forebrain (E15) was examined at 48h after the teratogen treatment. Although there was no staining of myelin basic protein (MBP), an oligodendrocyte marker (data not shown), the staining of NG2, a marker of oilgodendrocyte progenitor cells was detected. These cells showed a small size cell body in the btp of the control group (Fig. 4A). Blood vessels also appeared to be stained because of the presence of NG2 antigen in endothelial cells. At 48h after CP treatment, the NG2 positive oligodendrocytes showed very fine processes and increase in cell numbers (Fig. 4B).

Characterization of different cell types in the fetal forebrain exposed to CP using specific markers by Confocal microscopy

The gene expression profile prompted us to undertake a histological investigation to characterize the cell types that respond to CP treatment. In the forebrain

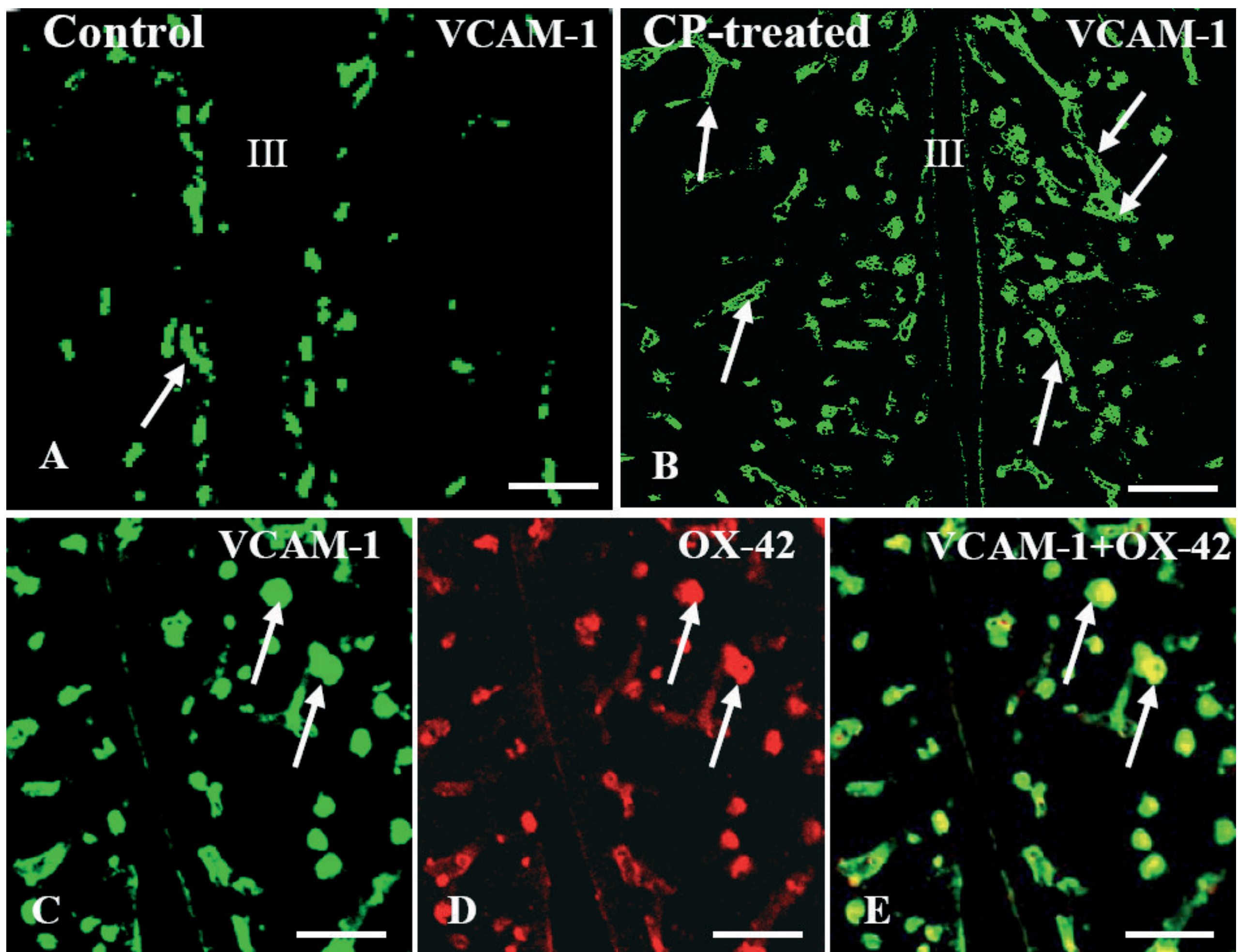

Fig. 6. Immunoreactivity of VCAM-1. In normal fetal forebrain, VCAM-1 immunolabeling (arrow) is detected only in the endothelial cells of parenchymal brain blood vessels in the proliferative zones **(A)**. In the experimental fetal rats treated with CP, VCAM-1 immunostaining in the blood vessels appears to be increased (arrows in **B**) and many VCAM-1 positive cells also exhibit OX-42 immunoreactivity (arrows in **C-E**). VCAM-1 immunofluorescence in **C** is in green. OX-42 immunofluorescence in D is in red. Arrows in **E** indicate cells that are double labeled by VCAM-1 (arrows, **C)** and OX-42 (arrows, **D**). Scale bar: 100 µm (A, B) and 200 µm (C-E).

of normal fetuses, Mash-1, a marker of relatively undifferentiated neuronal cells, was detected in the neuroepithelium associated with the lateral and the third ventricles (Fig. 5A). After CP treatment, Mash-1 staining appeared to be reduced (Fig. 5B). In addition, immunoreactivity of endothelial nitric oxide synthase (eNOS) was detected in the blood vessels around the third ventricle (Fig. 5C) of forebrain from normal fetuses. However, the intensity of its staining was reduced after CP treatment (Fig. 5D).

In normal fetuses, VCAM-1 immunolabeling was detected only in the endothelial cells of blood vessels in the proliferative zones of forebrain parenchyma (Fig. 6A). In fetuses treated with CP, VCAM-1 immunostaining in the blood vessels appeared to be enhanced (Fig. 6B). Furthermore, many amoeboid microglia labelled with a specific marker OX-42, in the vicinity of the blood vessels showed expression of VCAM-1 in the fetal forebrain of these CP-treated fetuses (Fig. 6C-E).

Colocalization studies using different antibodies were carried out using confocal microscopy to further characterize the AM/BM in both normal and CP-treated fetuses. In normal fetal forebrain, neither TNF-α nor TGF-ß staining was detectable. In the forebrain of CP-treated fetus, both TNF-α and TGF-ß positive cells were detected. Majority of these cells were OX-42 positive (Fig. 7A-C) or Lectin positive (Fig. 7D-F), indicating that AM/BM are the main cellular source of TNF-α and TGF-ß.

In order to confirm if immature neurons and other glial cells were involved in the inflammatory response after CP treatment, colocalization studies were carried out between MASH-1, NG2, vimentin and TNF-α. TNF-α immunoreactivity was induced in the developing forebrain of fetuses exposed to CP. After CP-treatment,

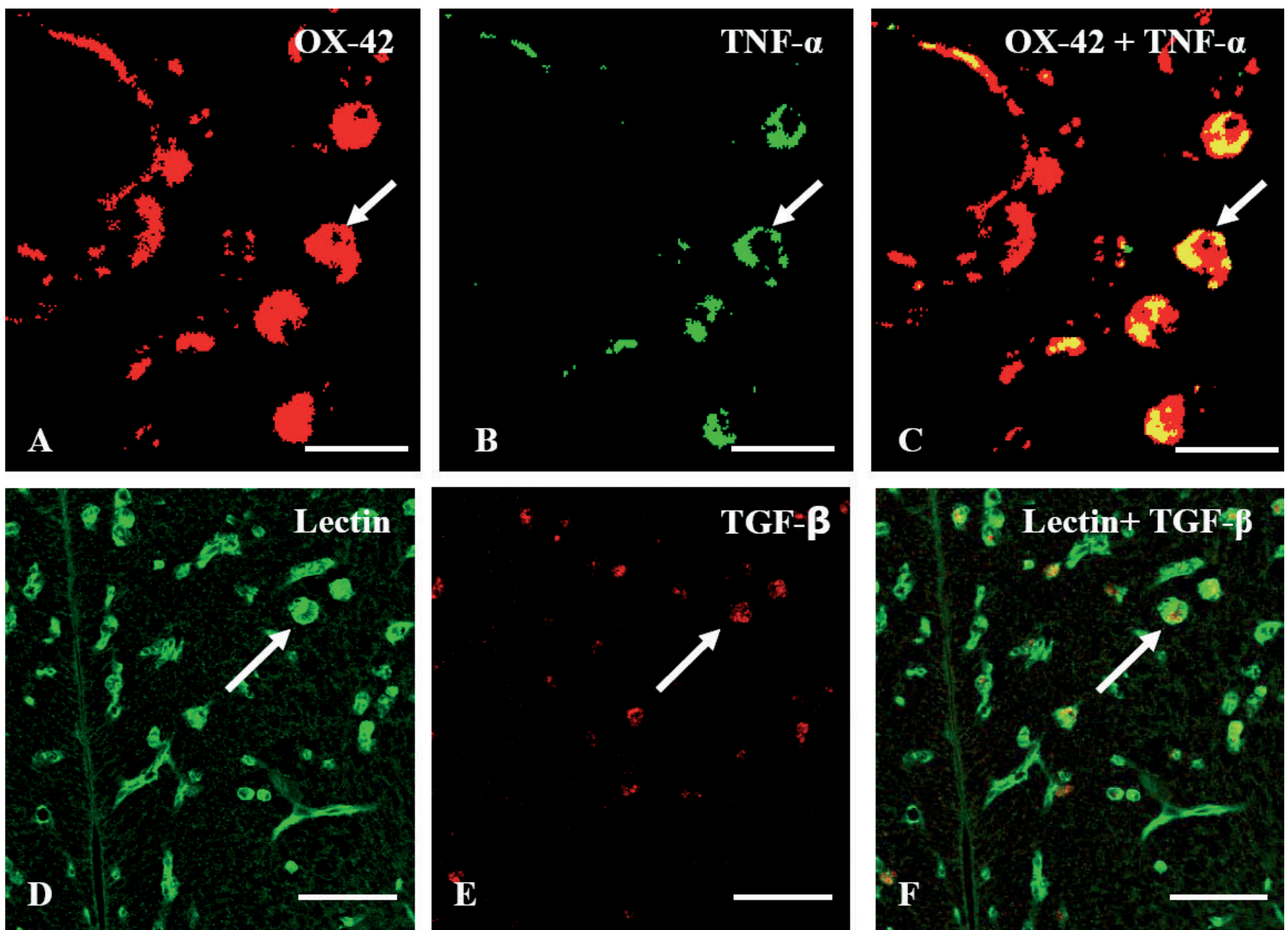

Fig. 7. Confocal images of OX-42/TNF-α and Lectin/ TGF-ß double immunolabeling in the dorsal neuroepithelium of diencephalon at 48 h after CP treatment. OX-42 immunofluorescence in A is in red. TNF-α immunofluorescence in **B** is in green. Arrow in **C** indicates the cell that is double labeled by TNF-α (arrow, **B**) and OX-42 (arrow, **A**). Lectin staining in **D** is in green. TGF-ß immunofluorescence in **E** is in red. Arrows in **D-F** show that Lectin positive microglia also exhibit TGF-ß immunoreactivity. Scale bar: 50 µm (A-C); 100 µm (D-F).

some Mash-1 positive cells displayed immunoreactivity of TNF-α (Fig. 8A-C). However, there were no NG2 positive oligodendrocyte progenitors exhibited TNF-α immunoreactivity (Fig. 8D-F). Vimentin is an intermediate filament protein expressed by radial glial cells with short processes in the fetal forebrain of both control and experimental group. The vimentin positive cells did not show TNF-α immunoreactivity (Fig. 8G-I).

Discussion

Neuropathological and brain imaging studies suggest that prenatal injury may result in neurodevelopmental defects. Cytoarchitectural studies also indicate cellular abnormalities suggesting of a disruption in neuronal connectivity, particularly in the proliferation areas around the ventricles in the forebrain (Padmanabhan, 1988, 1990). However, the molecular mechanisms underlying these findings remained unclear. In order to identify the molecular substrates associated with the neurodevelopmental defects following CP treatment, cDNA microarray analysis has been carried out to unravel a large set of genes that are differentially expressed in both experimental and control fetuses. The most remarkable change observed in the analysis was the differential expression of inflammation related genes suggesting that the excessive inflammatory response has an important role during the disease process in the fetal

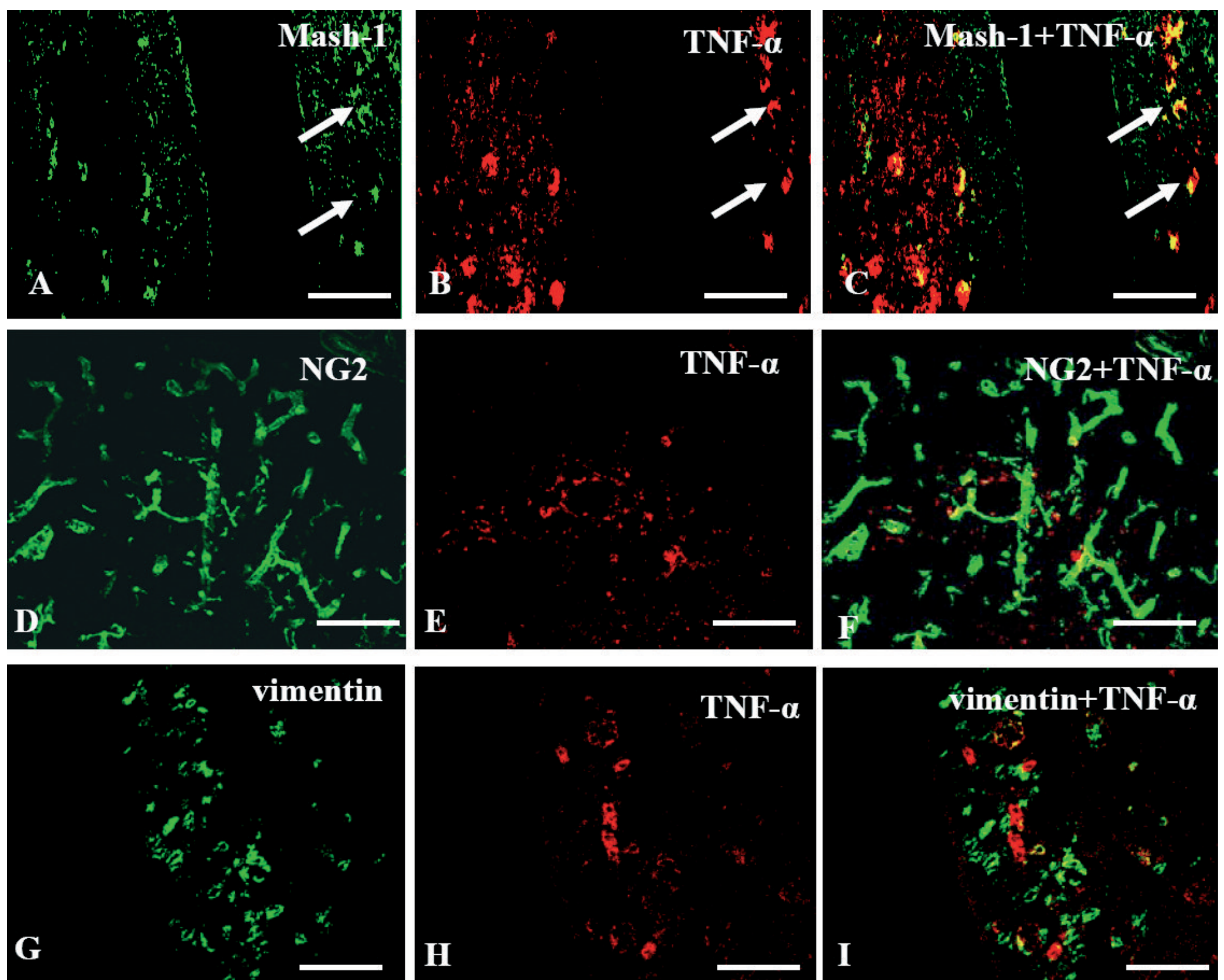

Fig. 8. Confocal images display the double immunolabeling of TNF-α with Mash-1, NG2, and vimentin in the dorsal neuroepithelium of diencephalon at 48 h after CP treatment. TNF-α immunofluorescence is in red. Mash-1, NG2, vimentin labelled cells are in green. In the control group, expression of TNF-α is hardly detectable (data not shown). In CP-treated group, some Mash-1 positive cells overlap with TNF-α immunoreactive cells (arrows in **A, B, C**). In contrast, NG2 (**D, E, F**) and vimentin (**G, H, I**) positive cells do not show TNF-α immunoreactivity. Scale bar: 50 μm.

brain.

The present study with CP-induced brain injury indicates that a cascade of acute injury responses including disturbances in the cerebral vasculature as manifested by the increase in VCAM-1 and E-selectin has been initiated. This could have resulted in microvascular endothelial activation, which has been shown to be important in the pathogenesis of a number of CNS diseases. One of the criteria for endothelial activation used in different studies is surface expression of a number of markers collectively termed endothelial cell activation antigens (Lee and Benveniste, 1999; Balabanov et al., 2001). Endothelial cell activation promotes inflammation through the upregulation of adhesion molecules such as VCAM-1 and E-selectin that facilitate the migration of lymphocytes and macrophages through the blood-brain barrier into the CNS (Kiss et al., 2001; Saliba and Henrot, 2001; Danton and Dietrich, 2003). It is conceivable that the increase in E-selectin (CD62) and VCAM-1 (CD106) observed in the present study following the brain injury induced by CP had elicited the influx of mononuclear cells into the fetal brain and subsequently aggravated the inflammation.

The elevation of chemoattractant cytokines and chemokines as shown by microarray analysis in the present study following CP treatment is also unequivocal. Members of α-family chemokines are chemotactic to granulocytes (gro) and ß-chemokines are mostly chemotactic to mononuclear cells such as monocytes and lymphocytes (Bona et al., 1999; Galasso et al., 2000; Anthony et al., 2001; Takami et al., 2001). In addition to their well-established role in the immune system, recent data suggest their involvement in the maintenance of CNS homeostasis in neuronal patterning during ontogeny and as potential mediators of neuroinflammation (Bacon and Harrison, 2000; Anthony et al,., 2001). Chemokines and their G protein-coupled receptors are constitutively expressed at low-to-negligible levels in various cell types in the brain. Their expression is rapidly induced by various neuro-inflammatory stimuli, implicating them in various neurological disorders such as trauma, stroke and Alzheimer's disease, in tumour induction and in neuro-immune diseases such as multiple sclerosis or acquired immunodeficiency syndrome (AIDS) (Galasso et al., 2000; Sun et al., 2000; De Groot and Woodroofe, 2001; Takami et al., 2001). Analysis of other relating factors that belong to chemokine family has revealed an induction and increase of mRNA expression of α and ß chemokines, MIP-1, MIP-2, gro and RANTES in the fetal brain exposed to CP. Chemokines, in conjunction with integrins and endothelial cell-adhesion molecules, are believed to control the migration of macrophages and leukocytes through tissues. Based on this information, it is suggested that the elevated expression of various chemokines in the fetal brain exposed to CP may be associated with NTD.

Cytokines are a heterogeneous group of polypeptide mediators that are associated with diseases and injuries in the CNS. In glial activation, the complex regulatory responses of the pro-inflammatory cytokine network are elicited (Benveniste, 1992). Generally in embryonic brain, expression level of cytokines appears to be low and undetectable, but is elevated in a disease state. Induced expression of cytokines including TNF-α and TGF-ß observed in the fetal brain exposed to CP confirm their involvement in abnormal neurodevelopment (Ivnitsky et al., 1998; Hao et al., 2001). In addition, expression of interleukin-1ß-converting enzyme (ICE/caspase-1) which is responsible for cleaving pro-IL-1ß to the biologically active IL-1ß has been found to be induced greatly in the fetal brain exposed to CP. ICE/caspase-1 and homologous proteases play a significant role in the developmentally regulated neuronal deaths (Milligan et al., 1995), suggesting that the elevated expression of ICE/caspase-1 may contribute to the developmental defects in the fetal brain exposed to CP.

Next, the involvement of NO in neuronal damage in the fetal brain injury after CP treatment should be considered. To date, three different isoforms of NOS have been characterized. It has been demonstrated that both neuronal NOS and inducible NOS activities are detrimental to the ischemic brain, whereas endothelial NOS plays a prominent role in maintaining the cerebral blood flow and prevents neuronal injury. It is proposed that increased iNOS expression in the fetal brain exposed to CP may contribute to fetal brain injury. On the other hand, down regulation of eNOS expression may compromise the neuroprotective effect and therefore further exacerbate the brain injury (Cobbs et al., 1997; Aguan et al., 1998; Bredt, 1999). In the present study there is an inconsistency in the detection of expression of some genes in the fetal brain by RT-PCR and microarray. Although RT-PCR results largely confirm the microarray data of the experimental group, expression of some of the cytokines, chemokines and iNOS was undetectable in the normal fetal brain by RT-PCR. This could be due to the fact that expression of these genes in normal fetal brain was at too low levels to be detected by the RT-PCR analysis.

Besides above factors, a number of proteases including elastase-like protease and metalloproteases also contribute to the initiation and maintenance of inflammation (Nakajima et al., 1992; Qiu et al., 1997). The cysteine protease, Cathepsin B which is produced by activated microglia, can degrade extracellular matrix proteins and induce neuronal apoptosis (Reddy et al., 1995; Bannerman et al., 1998; Kingham and Pocock, 2001). Markedly increased expression of Cathepsin B in the present study after CP treatment could be due to increased number of AM/BM and may be deleterious to the fetal brain, as it has been shown to induce neuronal apoptosis (Kingham and Pocock 2001).

Interestingly, the expression of genes involved in the normal neuronal activity appears to be down regulated in the fetal brain exposed to CP. Their down-regulation may disrupt the normal function of neurons leading to

cell death and subsequently NTD. The pattern of gene expression and histological evaluation confirmed the involvement of activated microglia in fetal brain injury following CP treatment. There is convincing evidence that microglia express both chemokines and chemokine receptors. Chemokines released by microglia may fulfill a dual role: firstly, in the trafficking of mononuclear phagocytes within the brain and, secondly, in mediating infiltration of the CNS by blood-borne monocytes (McManus et al., 1998; Gebicke-Haerter et al., 2001). All the above would have contributed directly or indirectly to the accumulation of AM / BM as observed in this study after CP treatment. A striking finding in this study was the up-regulated expression of proinflammatory cytokines, matrix metalloproteinases and free radicals (Benveniste, 1997; Possel et al., 2000; Gebicke-Haerter, 2001; Planas et al., 2001) genes in the experimental group. Expression of these genes was enriched particularly in AM/BM. In order to address the participation of other cell types in the inflammatory process, confocal microscopic analysis using markers for immature neurons, astrocytes and oligodendrocytes and pro-inflammatory cytokine antibodies was carried out. The results suggest that immature neurons could be involved in the inflammatory process whereas, the involvement of oligodendrocytes and astrocytes in this process is not definitive.

On the basis of our findings, we suggest an ongoing inflammatory response in the acute prenatal neurodegeneration and associated with this is an increased expression of many proteins involved in the complex inflammatory cascade. The inflammatory proteins include cytokines, chemokines, growth factors, enzymes, receptors and adhesion molecules. Along with this, the activated microglia also express potentially neurotoxic cytokines and proteases. This finding is of paramount importance since a therapeutic intervention may be targeted at the specific cytokines, chemokines or their receptors to reduce the inflammatory response that may be beneficial to the treatment of the teratogen induced prenatal disease.

Acknowledgements. This study was supported by research grants (R-181-000-077-112, R-181-000-038-112 and R-181-000-058-213) from the National University of Singapore and National Medical Research Council.

References

Aguan K., Murotsuki J., Gagnon R., Thompson L.P. and Weiner C.P. (1998). Effect of chronic hypoxemia on the regulation of nitric-oxide synthase in the fetal sheep brain. Brain Res. Dev. Brain Res. 111, 271-277.

Al Deeb S., Al Moutaery K., Arshaduddin M. and Tariq M. (2000). Vitamin E decreases valproic acid induced neural tube defects in mice. Neurosci. Lett. 292, 179-182.

Alizadeh A.A. and Staudt L.M. (2000). Genomic-scale gene expression profiling of normal and malignant immune cells. Curr. Opin. Immunol. 12, 219-225.

Alizadeh A.A., Eisen M.B., Davis R.E., Ma C., Lossos I.S., Rosenwald A., Boldrick J.C., Sabet H., Tran T., Yu X., Powell J.I., Yang L., Marti G.E., Moore T., Hudson J. Jr., Lu L., Lewis D.B., Tibshirani R., Sherlock G., Chan W.C., Greiner T.C., Weisenburger D.D., Armitage J.O., Warnke R., Levy R., Wilson W., Grever M.R., Byrd J.C., Botstein D., Brown P.O. and Staudt L.M. (2000). Distinct types of diffuse large B-cell lymphoma identified by gene expression profiling. Nature 403, 503-511.

Anthony D.C., Blond D., Dempster R. amd Perry V.H. (2001). Chemokine targets in acute brain injury and disease. Prog. Brain Res. 132, 507-524.

Bacon K.B. and Harrison J.K. (2000). Chemokines and their receptors in neurobiology: perspectives in physiology and homeostasis. J. Neuroimmunol. 104, 92-97.

Balabanov R., Goldman H., Murphy S., Pellizon G., Owen C., Rafols J. and Dore-Duffy P. (2001). Endothelial cell activation following moderate traumatic brain injury. Neurol. Res. 23, 175-182.

Bannerman D.D., Sathyamoorthy M. and Goldblum S.E. (1998). Bacterial lipopolysaccharide disrupts endothelial monolayer integrity and survival signaling events through caspase cleavage of adherens junction proteins. J. Biol. Chem. 273, 35371-35380.

Bennett G.D., Wlodarczyk B., Calvin J.A., Craig J.C. and Finnell R.H. (2000). Valproic acid-induced alterations in growth and neurotrophic factor gene expression in murine embryos [corrected]. Reprod. Toxicol. 14, 1-11.

Benveniste E.N. (1992). Inflammatory cytokines within the central nervous system: sources, function, and mechanism of action. Am. J. Physiol. 263, C1-16

Benveniste E.N. (1997). Role of macrophages/microglia in multiple sclerosis and experimental allergic encephalomyelitis. J. Mol. Med. 75, 165-173

Bona E., Andersson A.L., Blomgren K., Gilland E., Puka-Sundvall M., Gustafson K. and Hagberg H. (1999). Chemokine and inflammatory cell response to hypoxia-ischemia in immature rats. Pediatr. Res. 45, 500-509.

Bredt D.S. (1999). Endogenous nitric oxide synthesis: biological functions and pathophysiology. Free Radic. Res. 31, 577-596.

Brown P.O. and Botstein D. (1999). Exploring the new world of the genome with DNA microarrays. Nat. Genet. 21, 33-37.

Chabas D., Baranzini S.E., Mitchell D., Bernard C.C., Rittling S.R., Denhardt D.T., Sobel R.A., Lock C., Karpuj M., Pedotti R., Heller R., Oksenberg J.R. and Steinman L. (2001) The influence of the proinflammatory cytokine, osteopontin, on autoimmune demyelinating disease. Science 294, 1731-1735

Cobbs C.S., Fenoy A., Bredt D.S. and Noble L.J. (1997). Expression of nitric oxide synthase in the cerebral microvasculature after traumatic brain injury in the rat. Brain Res. 751, 336-338.

Craig J.C., Bennett G.D., Miranda R.C., Mackler S.A. and Finnell R.H. (2000). Ribonucleotide reductase subunit R1: a gene conferring sensitivity to valproic acid-induced neural tube defects in mice. Teratology 61, 305-313.

Danton G.H. and Dietrich W.D. (2003). Inflammatory mechanisms after ischemia and stroke. J. Neuropathol. Exp. Neurol. 62, 127-136.

De Groot C.J. and Woodroofe M.N. (2001). The role of chemokines and chemokine receptors in CNS inflammation. Prog. Brain Res. 132, 533-544

DeSesso J.M., Scialli A.R. and Holson J.F. (1999). Apparent lability of neural tube closure in laboratory animals and humans. Am. J. Med.

Genet. 87, 143-162.
Eisen M.B., Spellman P.T., Brown P.O. and Botstein D. (1998). Cluster analysis and display of genome-wide expression patterns. Proc. Natl. Acad. Sci. USA 95, 14863-14868.
Ferm V.H. and Hanlon D.P. (1986). Arsenate-induced neural tube defects not influenced by constant rate administration of folic acid. Pediatr. Res. 20, 761-762.
Galasso J.M., Miller M.J., Cowell R.M., Harrison J.K., Warren J.S. and Silverstein F.S. (2000) Acute excitotoxic injury induces expression of monocyte chemoattractant protein-1 and its receptor, CCR2, in neonatal rat brain. Exp. Neurol. 165, 295-305.
Gebicke-Haerter P.J. (2001) Microglia in neurodegeneration: molecular aspects. Microsc. Res. Tech. 54, 47-58.
Gebicke-Haerter P.J., Spleiss O., Ren L.Q., Li H., Dichmann S., Norgauer J. and Boddeke H.W. (2001). Microglial chemokines and chemokine receptors. Prog. Brain Res. 132, 525-532.
Grunblatt E., Mandel S., Maor G. and Youdim M.B. (2001). Gene expression analysis in N-methyl-4-phenyl-1,2,3,6-tetrahydropyridine mice model of Parkinson's disease using cDNA microarray: effect of R-apomorphine. J. Neurochem. 78, 1-12.
Hansen D.K., Barbee S.A., Grafton T.F., Gu Y. and Streck R.D. (2001). Antisense modulation of 5,10-methylenetetrahydrofo.late reductase expression produces neural tube defects in mouse embryos. Reprod. Toxicol. 15, 21-29.
Hao A.J., Dheen S.T. and Ling E.A. (2001). Response of amoeboid microglia/brain macrophages in fetal rat brain exposed to a teratogen. J. Neurosci. Res. 64, 79-93.
Ivnitsky I., Torchinsky A., Gorivodsky M., Zemliak I., Orenstein H., Savion S., Shepshelovich J., Carp H., Fein A. and Toder V. (1998). TNF-alpha expression in embryos exposed to a teratogen. Am. J. Reprod. Immunol. 40, 431-440.
Jin K., Mao X.O., Eshoo M.W., Nagayama T., Minami M., Simon R.P. and Greenberg D.A. (2001). Microarray analysis of hippocampal gene expression in global cerebral ischemia. Ann. Neurol. 50, 93-103.
Kingham P.J. and Pocock J.M. (2001). Microglial secreted cathepsin B induces neuronal apoptosis. J. Neurochem. 76, 1475-1484.
Kiss J.Z., Troncoso E., Djebbara Z., Vutskits L. and Muller D. (2001). The role of neural cell adhesion molecules in plasticity and repair. Brain Res. Rev. 36, 175-184.
Lee S.J. and Benveniste E.N. (1999) Adhesion molecule expression and regulation on cells of the central nervous system. J. Neuroimmunol. 98, 77-88.
McManus C.M., Brosnan C.F. and Berman J.W. (1998). Cytokine induction of MIP-1 alpha and MIP-1 beta in human fetal microglia. J. Immunol. 160, 1449-1455.
Milligan C.E., Prevette D., Yaginuma H., Homma S., Cardwell C., Fritz L.C., Tomaselli K.J., Oppenheim R.W. and Schwartz L.M. (1995). Peptide inhibitors of the ICE protease family arrest programmed cell death of motoneurons in vivo and in vitro. Neuron 15, 385-393.
Mirnics K. (2001). Microarrays in brain research: the good, the bad and the ugly. Nat. Rev. Neurosci. 2, 444-447.
Mody M., Cao Y., Cui Z., Tay K.Y., Shyong A., Shimizu E., Pham K., Schultz P., Welsh D. and Tsien J.Z. (2001). Genome-wide gene expression profiles of the developing mouse hippocampus. Proc. Natl. Acad. Sci. USA 98, 8862-8867.
Nakajima K., Shimojo M., Hamanoue M., Ishiura S., Sugita H. and Kohsaka S. (1992). Identification of elastase as a secretory protease from cultured rat microglia. J. Neurochem. 58, 1401-1408.
Padmanabhan R. (1988). Light microscopic studies on the pathogenesis of exencephaly and cranioschisis induced in the rat after neural tube closure. Teratology 37, 29-36.
Padmanabhan R. (1990). Electron-microscopic studies on the pathogenesis of exencephaly and cranioschisis induced in the rat after neural tube closure: role of the neuroepithelium and choroid plexus. Acta Anat. (Basel) 137, 5-18.
Pasinetti G.M. (2001). Use of cDNA microarray in the search for molecular markers involved in the onset of Alzheimer's disease dementia. J. Neurosci. Res. 65, 471-476.
Planas A.M., Sole S. and Justicia C. (2001). Expression and activation of matrix metalloproteinase-2 and -9 in rat brain after transient focal cerebral ischemia. Neurobiol. Dis. 8, 834-846.
Possel H., Noack H., Putzke J., Wolf G. and Sies H. (2000). Selective upregulation of inducible nitric oxide synthase (iNOS) by lipopolysaccharide (LPS) and cytokines in microglia: in vitro and in vivo studies. Glia 32, 51-59.
Qiu W.Q., Ye Z., Kholodenko D., Seubert P. and Selkoe D.J. (1997). Degradation of amyloid beta-protein by a metalloprotease secreted by microglia and other neural and non-neural cells. J. Biol. Chem. 272, 6641-6646.
Reddy V.Y., Zhang Q.Y. and Weiss S.J. (1995). Pericellular mobilization of the tissue-destructive cysteine proteinases, cathepsins B, L, and S, by human monocyte-derived macrophages. Proc. Natl. Acad. Sci. USA 92, 3849-3853.
Saliba E. and Henrot A. (2001). Inflammatory mediators and neonatal brain damage. Biol. Neonate 79, 224-227.
Seller M.J. and Bnait K.S. (1995). Effects of tobacco smoke inhalation on the developing mouse embryo and fetus. Reprod. Toxicol. 9, 449-459.
Sun D., Tani M., Newman T.A., Krivacic K., Phillips M., Chernosky A., Gill P., Wei T., Griswold K.J., Ransohoff R.M. and Weller R.O. (2000). Role of chemokines, neuronal projections, and the blood-brain barrier in the enhancement of cerebral EAE following focal brain damage. J. Neuropathol. Exp. Neurol. 590, 1031-1043.
Takami S., Minami M., Nagata I., Namura S. and Satoh M. (2001). Chemokine receptor antagonist peptide, viral MIP-II, protects the brain against focal cerebral ischemia in mice. J. Cereb. Blood Flow Metab. 21, 1430-1435.
Whitney L.W., Becker K.G., Tresser N.J., Caballero-Ramos C.I., Munson P.J., Prabhu V.V., Trent J.M., McFarland H.F. and Biddison W.E. (1999). Analysis of gene expression in mutiple sclerosis lesions using cDNA microarrays. Ann. Neurol. 46, 425-428.

Accepted January 15, 2007